Journal of Operation and Automation in Power Engineering
Vol. 1, No. 2, Summer & Fall 2013, Pages: 147-155
http://journals.uma.ac.ir/joape

Flexible Power Electronic Transformer for Power Flow Control Applications

J. Fallah Ardeshir[1]*, A. Ajami[2], A. Jalilvand[3], A. Mohammadpour[1]

[1] Department of Electrical Engineering, University of Tabriz, Tabriz, Iran.
[2] Department of Electrical Engineering, Azarbaijan Shahidmadani University, Tabriz, Iran.
[3] Department of Electrical Engineering, University of Zanjan, Zanjan, Iran

ABSTRACT

This paper proposes a Flexible Power Electronic Transformer (FPET) for the application in the micro-grids. The low frequency transformer is usually used at the Point of Common Coupling (PCC) to connect the low voltage grid and utility network to each other. The conventional 50Hz transformer results in enhanced low voltage-grid power management system during grid-connected operation. In this paper, the whole system represented as two, three-phase AC systems with an intermediate high-frequency transformer for power flow controlling. The FPET consists of a high frequency transformer and three-phase to single-phase matrix converter. The matrix converters are modulated with a Pulse Width Modulation (PWM) strategy for a bi-directional power flow control. Phase shift modulation strategy in two sides of FPET is used for power flow controlling by PI controller from utility network to low voltage grid and vice versa. FPET model is established in Matlab/Simulink software with controller for power flow controlling. Presented simulation results have shown the validity of the proposed control system for FPET through the Matlab/Simulink simulation.

KEYWORDS: Flexible Power Electronic Transformer (FPET), Matrix Converter, Bidirectional Power Flow Control.

1. INTRODUCTION

Distribution power transformers are used in the power grid to implement the voltage conversion, isolation and noise decoupling. They are very reliable and sensitive to harmonics. On the other hand, due to their large iron cores, they are bulky, massive and expensive devices. Their oil threats the environment [1-4]. The power electronic transformers have introduced to carry out voltage transformation, isolate the loads from grid and improve the power quality. High frequency transformer used in FPET to makes the system lighter and smaller. Since flux density is inversely proportional to frequency, the frequency has increased to reduce the transformer size. Some of FPET qualities and applications are voltage sag compensation, instantaneous voltage regulation, high reliability, power factor correction and power quality improvement of distribution system [5]-[18]. In recent years, several structures of FPET presented [6-9].

A transformer less AC/AC buck converter, which is capable of voltage level conversion, has been proposed in [2]. The high voltage stress on semiconductor devices is its main drawback. The second topology [9, 14, 5] are three fundamentals stages: an input, an isolation and an output. This topology achieves high power quality and desired output voltage with a DC link and several power electronic converters [5, 15, 19]. In another topology of PET, AC waveform side of utility network modulated

Received: 6 Jule 2013 Revised: 21 Aug. 2013
Accepted: 6 Oct. 2013
* Corresponding author:
J.F.Ardeshir (E-mail: j.fallah@tabrizu.ac.ir)

with a PWM strategy in to a High Frequency (HF) square wave. This square wave demodulated to AC waveform by switching of matrix converter at secondary of transformer.

The FPET consist of matrix converter that contributed to the high frequency operation. The matrix converter is a direct AC/AC power converter and uses a matrix of semiconductor bidirectional switches. The matrix converter is allowing the generation of sinusoidal variable voltage and variable frequency. The matrix converter has many advantages and features which are described in [7-9]. They are as follows: no bulky DC link capacitor, ability to make sinusoidal input current and compact circuit design with high efficiency.

The main point of FPET with matrix converter is reduces stages and components the three parts of FPETs. The primary purpose is to reduce the size, weight, cost and improve efficiency. In this paper, the active and reactive power flow can been controlled between two grids to determine desired value at the PCC.

The FPET is comprised of a high frequency step down transformer and three-phase to single-phase matrix converters. Figure 1 shows single line diagram of two three-phase AC systems with an interface high frequency transformer AC link. A PI controller has designed for the active and reactive power flow at the PCC. Simulation results are presented confirmation the operation. The modules have connected to a common DC link that facilitates energy transfer between modules [22-23]. They need DC link capacitors and many power electronic converters. In this paper, we use FPET that can control the power flow with fast response and not required DC link between two grids. Unlike the papers [22] and [23], we can control power flow between two grids by controlling the pulse duration and phase shift of pulses between two sides of FPET.

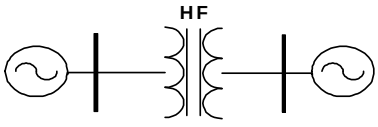

Fig.1. Line diagram of system

2. TOPOLOGY ANALYSIS

The FPET consists of a high frequency transformer and converters three phase to single phase at the primary (side of high voltage) and secondary of transformer (side of low voltage). The whole system as shown in Fig. 2 includes two matrix converters with high frequency AC link and this is whole the system. Three phases input AC voltage has converted into high frequency single-phase voltage. The output side converter consists of a three phase to single phase matrix converter, thus yielding high frequency pulsating single phase AC voltages at the primary and secondary of high frequency transformer. The switching frequency of the FPET ranges within 10-20 kHz. The switching frequency should be chosen greater than the input and output frequencies to avoid the generation of low order harmonics. The primary side of AC source is the utility while the secondary side of AC source is the utility with different amplitudes. The three-phase input AC voltage at the line frequency (60 Hz) has converted into high frequency (10 kHz) single-phase voltage with the input side of matrix converter. In the secondary side, three phase input AC voltage converter is a three phase to single-phase matrix converter. This yields high frequency pulsating single-phase AC voltage at the primary and secondary of the high frequency transformer with leakage reactance L.

The side of high voltage has a three phase input AC voltage source with peak magnitude v_{inH} and angular frequency w_{inH} according with (1). The two sides of transformer consists of a high frequency transformer with three phase to single phase matrix converter. The switching application is running between modes that generate maximum voltage at the input and the output voltage waveform. These waveforms generated by the sampled pieces of the input voltage waveforms [20]. Clearly, min $v_{in}(t)$ and max $v_{in}(t)$ explain the voltage lower and upper

bands each mode according to Tables 1. The duty ration switches are a function of $(M(t))$ which are varying time signals with desired output frequency. f_s The time varying signals $(M(t))$ for matrix converter are gives by (2).

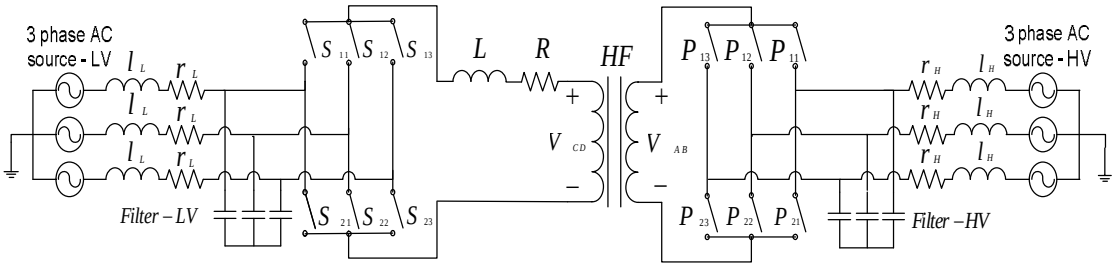

Fig. 2. Topology of system

$$v_{iaH}(t) = V_{iH}\sin(w_{inH})$$
$$v_{ibH}(t) = V_{iH}\sin(w_{inH} - \frac{2\pi}{3}) \quad (1)$$
$$v_{icH}(t) = V_{iH}\sin(w_{inH} - \frac{4\pi}{3})$$

$$M(t) = \begin{cases} K; & 0 \le t \le t_p + t_d \\ -K; & t_p \le t \le t_p + t_d \\ K; & t_p + t_d \le t \le T_s \end{cases} \quad (2)$$

The bidirectional switches of the matrix converter are modulated at 10 KHz switching frequency and modulation index K is 1. The t_p is a phase shift between the voltages, and the t_d is duty cycle of the voltage at transformer primary and secondary side of transformer. The t_p is used for active power flow control and t_d is used for reactive power flow control. The condition for the phase shift follows $0 \le t_p \le T_s$.

Figure 3 also shows the modulation signal of the input and output side of matrix converters where the phase-shift is given by $(2\pi t_p/T_s)$ radians and power flow can be adjusted by these signals.

Figure 4 shows desired output voltage has generated byusing sampled pieces from maximum instantaneous magnitudes of the input voltageswith six switches of converter [20].

The single-phase pulsating output voltages are gives by V_{AB} and V_{CD} in side of high voltage and low voltage, respectively. The possible modes sides of high voltage is summarized in Table 1. The matrix converter has six bi-directional switches are shown with P_{11}, P_{12} and P_{13} corresponding with output phase A and P_{21}, P_{22} and P_{23} corresponding with output phase B.

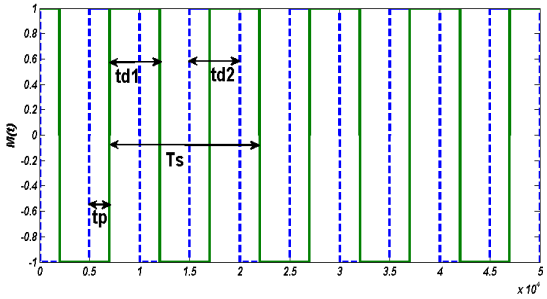

Fig. 3. Control signals for matrix converter modulation

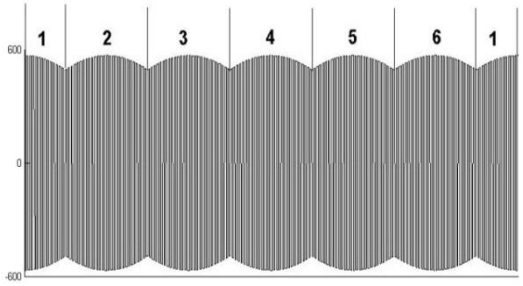

Fig. 4. Control method for three-phase to single-phase matrix converter with six switches.

The possible modes sides of low voltage are similar with side of high voltage. The single-phase high frequency pulsating voltage assesses as (3) & (4) at primary and secondary side of transformer.

$$V_{pri}(t) = v_{inH}\left(1-\frac{2t_d}{T_s}\right) + \frac{2v_{inH}}{T_s}\sum_{n=1}^{\infty}\left(\frac{1}{n}\left(-\sin\frac{2n\pi}{T_s}t_d\right)\cos\left(\frac{2n\pi}{T_s}t\right) + \left(\cos\frac{2n\pi}{T_s}(t_d)-1\right)\sin\left(\frac{2n\pi}{T_s}t\right)\right) \quad (3)$$

$$V_{\sec}(t) = v_{inL}\left(1-\frac{2t_d}{T_s}\right) + \frac{2v_{inL}}{T_s}\sum_{n=1}^{\infty}\left(\frac{1}{n}\left(\sin\left(\frac{2n\pi}{T_s}t_p\right)-\sin\frac{2n\pi}{T_s}(t_p+t_d)\right)\times\cos\left(\frac{2n\pi}{T_s}t\right)+\left(\cos\frac{2n\pi}{T_s}(t_p+t_d)-\cos\frac{2n\pi}{T_s}t_p\right)\times\sin\left(\frac{2n\pi}{T_s}t\right)\right) \quad (4)$$

In these equations, v_{inH} and v_{inL} are the peak voltages three phase input AC sources and f_s is the switching frequency. The line current can be supposed to be a square wave at the primary side of transformer and the input line current is in phase with the input voltage at the primary side of transformer.

Table 1. States modes for three-phase to single phase matrix converter with six switches

mode	On switches	V_{AB}
1	P_{11} & P_{22}	$v_a - v_b$
2	P_{12} & P_{23}	$v_b - v_c$
3	P_{13} & P_{21}	$v_c - v_a$
4	P_{12} & P_{21}	$v_b - v_a$
5	P_{13} & P_{22}	$v_c - v_b$
6	P_{11} & P_{23}	$v_a - v_c$

3. PI CONTROLLER FOR POWER CONTROL

The simplified of system is shown in Fig. 5, where the high frequency transformer is represented by its inductance and series resistance. This system is model as two line frequency AC sources with high frequency AC link. The primary side of AC source is utility and the secondary side of AC source is another source with phase shift t_p between them. The power flow between two AC systems is achieves with phase shift technique similar to a dual active bridge for a DC system. The essential component of single-phase high frequency pulsating voltage eat the primary and secondary of transformer can evaluated with (5) and (6).

$$V_{AB}(t) = v_{inL}\left(1-\frac{2t_d}{T_s}\right) + \frac{2v_{inL}}{\pi}\left(\sin\left(\frac{2\pi}{T_s}t_p\right)-\sin\left(\frac{2\pi}{T_s}(t_d+t_p)\right)\times\cos\left(\frac{2\pi}{T_s}t\right)+\left(\cos\frac{2\pi}{T_s}(t_p+t_d)-\cos\frac{2\pi}{T_s}t_p\right)\times\sin\left(\frac{2\pi}{T_s}t\right)\right) \quad (5)$$

$$V_{CD}(t) = v_{inH}\left(1-\frac{2t_d}{T_s}\right) - \frac{2v_{inH}}{\pi}\left(\left(\sin\left(\frac{2\pi}{T_s}t_d - t\right)+\sin\frac{2\pi}{T_s}t\right)\right) \quad (6)$$

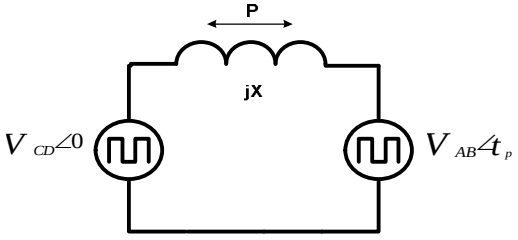

Fig.5. Simplified AC system

For shifted square voltages on the primary and secondary side of transformer between two phases, the active power flow can controlled by controlling the phase shift t_p. The bi-directional active and reactive power can defined as follows:

$$P = \frac{V_{AB}\,V_{CD}}{X}\sin(t_p) \quad (7)$$

$$Q = \frac{V_{AB}}{X}(V_{AB} - V_{CD}\cos t_p) \quad (8)$$

The regulated phase shift angle according to the desired active power limit is setting by the utilities. This achieved with PSO algorithm by a PI controller to produce the control signal applied for matrix converter modulation. The PI controller has been designed with proportional gain K_P and integral gain K_I. The K_P and K_I

adjusted by PSO algorithm are supplying a faster response to obviation any steady state error according to (9). The active and reactive power transfer function, given by (7) & (8) being a nonlinear equation is by linear over operating point θ_0 and δ_0 to define the power stage of the system, given by (10) and (11). As (7) and (8) are nonlinear equation and set of parameters is difficult, so the K_P and K_I are adjusted by PSO algorithm [21].

$$G(s) = \frac{K_P s + K_I}{s} \tag{9}$$

$$G_P = \frac{V_H V_L}{X} \cos\theta_0 \tag{10}$$

$$G_Q = \frac{V_{CD}}{X} \sin\delta_0 \tag{11}$$

4. POWER FLOW CONTROL

The active power flow is bi-directional between two utilities. The utilities set the reference limit of the active and reactive power. As shown in Fig. 6, the PI controller of active and reactive powerare provides with PSO algorithm to modulation signal of the primary and secondary sides of matrix converter. The active power flow between the primary and secondary side of transformer have controlled by adjusting the phase shift (t_p) and the reactive power flow control achieved by controlling the duty cycle (t_d) as (10) and (11). To have continuous power flow, the current primary and secondary winding is a square waveform. The active power flow control is achieved by controlling the parameter t_p as defined by modulating signals at a predefined limit (P_{ref}) and the active power flow control (Q_{ref}) is achieved by controlling the t_d.

The average active power has measured at the output AC source and be restricted by calculating correspond modulation signal for the secondary side of matrix converter and the equivalent phase shift can be achieved.

To acquire an optimal combination, this paper employs PSO algorithm to improve optimization synthesis and find the global optimum value of fitness function. In this paper, an Integral of Time multiplied Absolute value of the Error (ITAE) is taken as the objective function. The objective function is defined as follows:

$$J = \int_0^{t_{sim}} t.(\left|P_{ref} - P_{real}\right| + \left|Q_{ref} - Q_{real}\right|)dt \tag{12}$$

$$F = \sum_{i=1}^{N_p} J_i \tag{13}$$

In the above equations, t_{sim} is the time range of simulation and N_P is the total number of operating points that the optimization carried out at these points. In This paper, the active and reactive powers have been considered in the interval 0-1 p.u. and this interval is divided to 20 equal parts (N_P =20). It is noticeable that the increasing N_P is caused the accuracy of optimization is increased.

The ITAE performance index has the advantages of producing smaller overshoots and oscillations than the Integral of the Absolute Error (IAE) or the ISE (integral square error) performance indices [24].

For objective function calculation, the timedomain simulation of the test power system carried out for the simulation period. It aimed to minimize this objective function to improve the system response in terms of the settling time and overshoots. As regards, the controller gains determine the cost of control system, so the upper and lower limits of controller gains considered as constraints. The design problem can formulated as the following constrained optimization problem, where the constraints are the controller parameters bounds:

Minimize F Subject to:

$$K_p^{\min} \le K_p \le K_p^{\max} \tag{14}$$
$$K_i^{\min} \le K_i \le K_i^{\max}$$

Typical ranges of the optimized parameters are [0.01-5] for K_P and 0.01-200 for K_I. The proposed approach employs PSO algorithm to solve this optimization problem and search for an optimal set of output feedback controller parameters. The PSO algorithm and its improvement methods described in several published literatures. Application of PSO algorithm in power systems has been reported

in several papers and its effectiveness has been proved [25, 26]. Figure 6 shows the flow chart of the PSO algorithm. The update velocities and positions of particles are done by (15) and (16) in this flowchart.

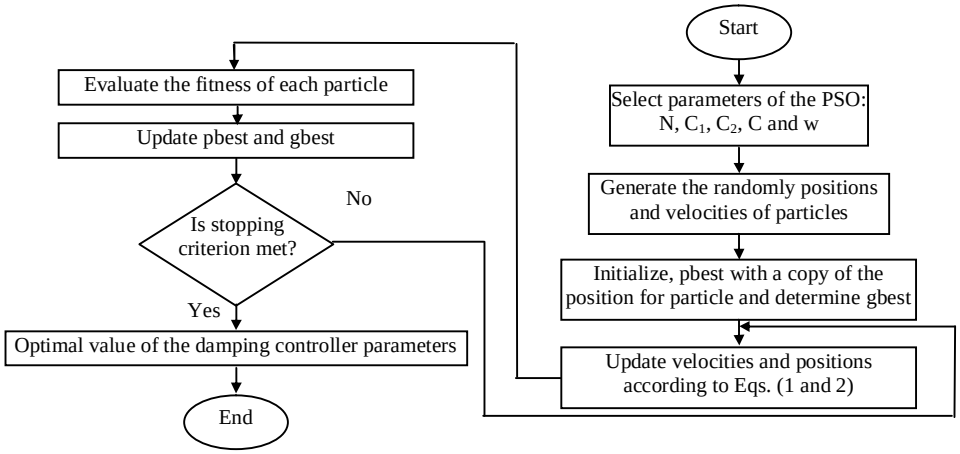

Fig. 6. Flowchart of the PSO technique.

$$v_{id} = w \times v_{id} + c_1 \times rand(\,) \times (P_{id} - x_{id}) + c_2 \times rand(\,) \times (P_{gd} - x_{id}) \quad (15)$$

$$x_{id} = x_{id} + v_{id} \quad (16)$$

In above equations, the parameters used is defined in [26].

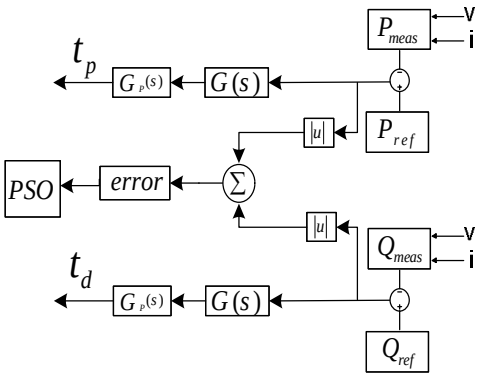

Fig. 7. Control System of active and reactive power

Figure 7 shows an error vectors and the chart flow. In this equation, T_S shows the duration of simulation. The error 1 and error 2 are error between real and measured parameters of active and reactive power respectively. In this method, the coefficients are becomes high and low to set the parameters with try and error method.

5. SIMULATION RESULTS

The FPET model and total system has established in Matlab/Simulink software. Several numerical simulations analysis are shown in Figs. 8-12. In this simulation, the high voltage side of the FPET has connected with RMS magnitude 20 kV three-phase distribution system. Its high voltage side of the FPET has connected with RMS magnitude the 400V three-phase distribution system. The high frequency pulsating AC voltage at transformer primary and secondary is a square wave as shown in Fig. 8 and phase shift is apparent between them. The active power flow can adjust by controlling the phase shift. Figure 9 shows voltage and current side of the high frequency pulsating AC voltage at secondary of transformer and clearly that the input line current is in phase with input voltage. Figure 10 shows voltage and current side of secondary transformer. The control strategy of FPET operation allows to control over the phase shift between the input current and input voltage of the matrix converter. This in turn allows to control of the reactive power. Figures 11 and 12 gives the profile of average active and reactive power flow at various instances with different phase shifts and duty cycles as determined with control system. These figures are showing the simulation results when the reference of the active and reactive power has changed from one grid to another grid and system follows the reference values.

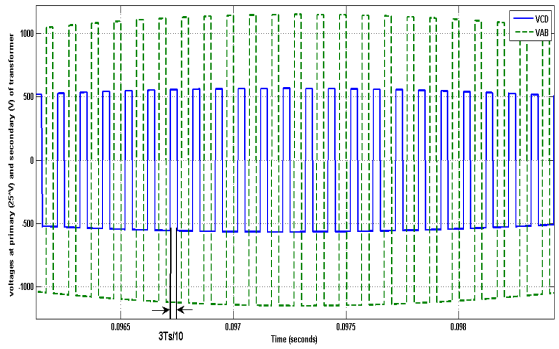

Fig. 8. Phase shift between voltages at primary and secondary of transformer

Table 2. Parameters of simulation

Parameters	Value
Input phase voltage side of High voltage	20KV RMS
Input phase-phase voltage side of Low voltage	400V RMS
Power frequency	60HZ
MF transformer	20000:400,10KHz, 900 KVA
Matrix converter switching frequency	10 KHZ

Figure 12 indicates the variation in the reactive power at the low voltage grid side of matrix converter through a step change in the phase shift between the input current and input voltage of the matrix converter as shown in Fig. 10. The result of input voltage and current is shown in Fig. 10. When the modulation strategy is employed a phase shift, the resulting shift is illustrated in input current. The parameters value of simulations is shown in Table 2.

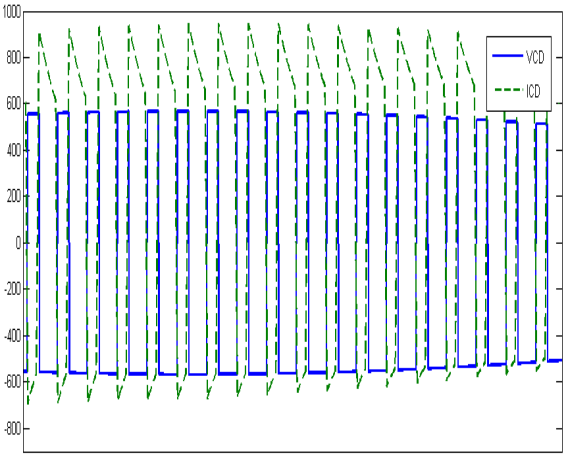

Fig. 9. Voltages and current at secondary of transformer

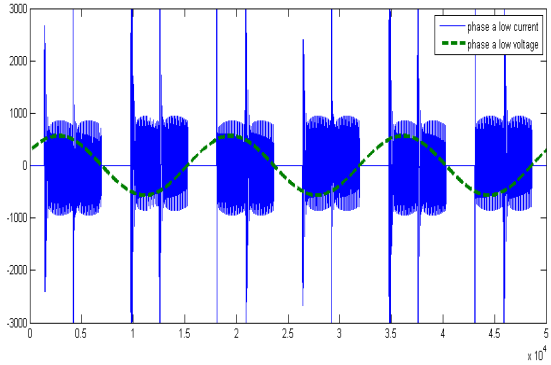

Fig. 10. Voltages and current of phase A at secondary of transformer

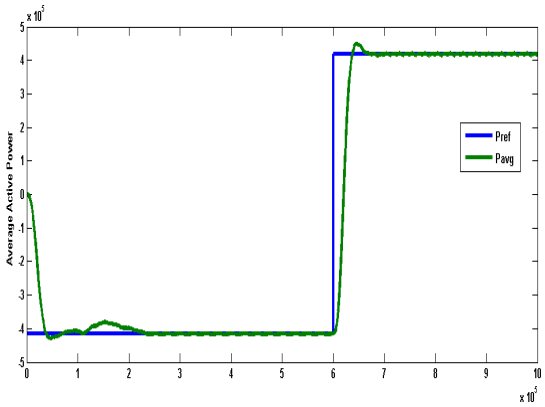

Fig. 11. Step response of average active power

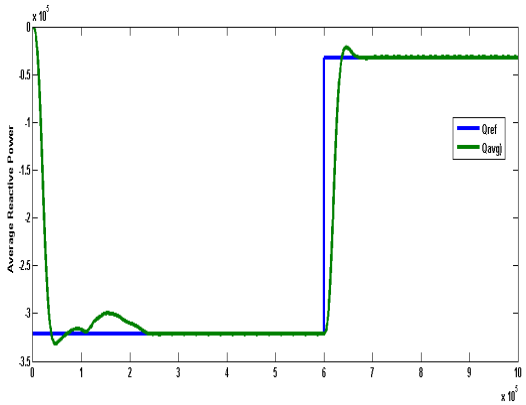

Fig. 12. Step response of average reactive power

6. CONCLUSION

The FPET and controller of system play animportant role in optimal operation. A FPET has studied for its size and weight advantages over conventional transformer. In this paper, the FPET was proposed for application in power distribution system. This study extends the application of the FPET for bidirectional power flow control between the utility and low voltage

grid. The FPET could control power flow between two grids with fast response and it was not required dc link (matrix converter). Three - phase to single-phase matrix converter provides high frequency operation of FPET. Bidirectional power flow was achieved between the two three phase AC systems. FPET could be controlled by the active and reactive power flow to a desired value determined with controller at the PCC. The parameters of PI controller were tuned with PSO algorithm. The simulation results were shown when the reference of the active and reactive power is changing from one grid to another. These results substantiated the capability of the FPET to control the active and reactive power that injected into the two sides of FPET.

REFERENCES

[1] W. Mcmurray "Power converter circuits have a high frequency link," *U.S. Patent 3517300*, 1970.

[2] K. Harada, F. Anan, M. Jinno, Y. Kawata, T. Nakashima, K. Murata and H. Sakamoto, "Intelligent transformer," *Proceedings of the 27th Annual IEEE Specialists on Power Electronics*, pp. 1337-1341, 1996.

[3] K. Harada, H. Sakamoto and M. Syoyama, "Phase controlled dc–ac converter with high-frequency switching," *IEEE Transactions on Power Electronics*, vol. 3, pp. 406-411, 1988.

[4] V. John and N. Mohan "Standby power supply with high-frequency isolation," *Proceedings of the 10th Annual APEC on Power Electronics*, pp. 900-994, 1995.

[5] Z. Wangand and K. Yu, "The research of power electronic transformer (PET) in smart distribution network," *Proceedings of the International Conference on Power System Technology*, pp.1-7, 2010.

[6] S. Srinivasan and G. Venkataramanan, "Comparative evaluation of PWM AC-AC converters," *Proceedings of the 26th IEEE Power Electronic Specialist Conference*, pp. 529-535, June,1995.

[7] H. Krishnaswami and V. Ramanarayanan, "Control of high frequency ac link electronic transformer," *IET Electric Power Applications*, vol. 152, no. 3, pp. 509- 516, 2005.

[8] E.R. Ronan, S.F.Glover and D.L. Galloway "A power electronic-based distribution transformer," *IEEE Transactions on Power Delivery*, vol. 17, pp. 537-543, 2002.

[9] S.H. Hosseini,M. Sabahi, M.B.B. Sharifian, A.Y. Goharrizi and G.B. Gharehpetian, "Bi-directional power electronic transformer based compact dynamic voltage restorer," *Proceedings of the IEEE Power & Energy Society General Meeting*, pp.1-5, 2009.

[10] H. Imaneini and Sh. Farhangi, "Analysis and design of power electronic transformer for medium voltage levels," *Proceedings of the IEEE International Conference on Power Electronic Specialist*, pp.1-5, 2006.

[11] H. Iman-Eini, J.L. Schanen, Sh. Farhangi, J. Barbaroux and J.P. Keradec, "A power electronic based transformer for feeding sensitive loads," *Proceedings of the IEEE International Conference on Power Electronic Specialist*, pp. 2549-2555, 2008.

[12] D. Wang, C. Mao, J. Lu, S. Fan and F. Peng, "Theory and application of distribution electronic power transformer," *Electric Power Systems Research*, vol. 77, pp. 219-226, 2007.

[13] D. Wang, C. Mao and J. Lu "Coordinated control of EPT and generator excitation system for multidouble-circuit transmission-lines system," *IEEE Transactions on Power Delivery*, vol. 23, pp. 371-379, 2008.

[14] H. Liu, C. Mao, D. Wang, "Optimal regulator-based control of electronic power transformer for distribution systems," *Electric Power Systems Research*, vol. 79, pp. 863-870, 2009.

[15] M.R. Banaei, S.H. Hosseini, S. Khanmohamadi and G.B. Gharehpetian, "Verification of a new energy control strategyfor dynamic voltage restorer by simulation," *Simulation Modeling Practice and Theory*, vol. 14, no. 2, pp. 112-125, 2006.

[16] M. Haque, "Compensation of distribution system voltage sag by DVR and D-STATCOM," *Proceedings of IEEE Conference on Power Technology*, pp. 1336-1340, *Porto*, 2001.

[17] D. Dujić, F. Kieferndorf and. F. Canales, "Power electronic transformer technology for traction applications an overview," *Proceedings of the 7th International Conference on Motion Control*, pp. 4638-4645, 2012.

[18] M.R. Banaei and E. Salary, "Power quality

improvement based on novel power electronic transformer", *Proceedings of the Second Conference on Power Electronics, Drive Systems and Technologies*, pp. 286-291, 2011.

[19] E. Babaein, "A new PWM based control method for forced commutated cycloconverters," *Energy Conversion and Management*, vol. 53, pp. 305-313, 2012.

[20] R.C. Eberhart and Y. Shi, "Particle swarm optimization: developments, applications and resources", *Proceedings of the IEEE Congress on Evolutionary Computation*, vol. 1, pp. 81-86, 2001.

[21] M. Sabahi, A.Y. Goharrizi, S.H. Hosseini, M.B.B Sharifian and G.B Gharehpetian, "Flexible power electronic transformer," *IEEE Transactions on Power Electronics*, vol. 25, no. 8, pp. 2159-2169, 2010.

[22] C. Rajesh, M. Kishor and N.P. Chandrao, "Reduced switch topology of power electronic transformer," *International Journal of Engineering Research and Applications*, vol. 2, pp. 2786-2792, 2012.

[23] D. Maiti, A. Acharya and Mithun, "Tuning PID Controllers using the integral time absolute error criterion," *Proceedings of the 4th Information and Automation for Sustainability on Power Electronics Conference*, pp. 457-462, 2008.

[24] J. Kennedy, R. Eberhart and Y. Shi, "Swarm intelligence," *Morgan Kaufmann Publishers*, San Francisco, vol. 3, pp. 95, 2001.

[25] M. Clerc and J. Kennedy, "The particle swarm explosion, stability, and convergence in a multidimensional complex space," *IEEE Transactions on Evolutionary Computation*, vol. 6, no. 1, pp. 58-73, 2002.